

Supporting information

Selective Recognition of Lithium (I) Ions using Biginelli based Fluorescent Organic Nanoparticles in aqueous medium

Gaganpreet Kaur^a, Amanpreet Singh,^b P. Venugopalan,^c Navneet Kaur^{*a,c}, Narinder Singh^{*b}

^aCentre for Nanoscience & Nanotechnology (UIEAST), Panjab University Chandigarh 160014, India.

^bDepartment of Chemistry, Indian Institute of Technology Ropar, Rupnagar, Punjab 140001, India.

^cDepartment of chemistry, Panjab University, Chandigarh, 160014, India.

*Corresponding authors.

Table of contents

Figure S1. (a) The absorbance and (b) the excitation spectra of compound 1 (5 μM) in DMSO and its nanoparticles, ONP (5 μM) in water.

Figure S2. Changes in emission profile of ONP (5 μM) in water upon addition of 50 μM of particular metal nitrate salts (a) in absence of buffer (b) in presence of HEPES buffer, pH 7.4.

Figure S3. Fluorescence spectra of **ONP** (a) before Li (I) binding (b) after Li (I) binding at different time intervals. (c) Absorbance spectra of ONP at different time intervals.

Figure S4. (a) Absorbance spectra of ONP upon titration with Li (I); (b) Excitation spectra of ONP upon titration with Li (I)

Figure S5. DLS histogram of ONP on interaction with (a) Li (I), 30 nm (b) Cs (I), 25 nm (c)Cr (III), 26nm (d) Al (III), 25 nm (e) Zn (II), 26 nm.

Figure S6. Competitive experiment (a) in absence of buffer (b) in presence of HEPES buffer, pH 7.4.

Figure S7. Fluorescence spectra of **ONP** at different pH values (a) acidic medium (b) basic medium (c) Fluorescence intensity vs pH profile (d) Absorbance spectra of **ONP** at different pH values.

Figure S8. (a) DLS at pH=4.1, 25nm (b) DLS at pH= 8, 23nm (c) DLS at pH= 11, 25nm

Figure S9. Fluorescence spectra of **ONP** on addition of different concentrations of tetrabutylammonium perchlorate to evaluate the salt effect.

Figure S10. Packing diagram of 1.

Figure S11. (a) ¹H-NMR (b) ¹³C-NMR of compound 1.

General information

The required chemicals and reagents were procured from Sigma-Aldrich and were of analytical grade. TLC was performed on glass plates coated with (Kieselgel 60 PF254, Merck) silica gel. The CHN analysis was executed on a Perkin Elmer 2400 CHN Elemental Analyser. The UV-Vis absorption spectra were monitored on a SpectroScan 30 spectrophotometer in a quartz cell having 1 cm path length. The fluoremetric experiments were performed on Shimadzu RF-5301 spectrofluorophotometer in a quartz cuvette. The average particle size of nanoparticles was analyzed with dynamic light scattering, DLS using the external probe feature of MetrohmMicrotrac Ultra Nanotracs Particle Size Analyzer. The TEM images were obtained from a Hitachi (H-7500) transmission electron microscope instrument working at 120 kV with a resolution of 0.36 nm (point to point) and 40–120 kV operating voltage. Sample for TEM was prepared on a 400-mesh, carbon-coated copper grid. The X-ray diffraction data was obtained on a Bruker X8 APEX II KAPPA CCD diffractometer (at 100 K) which used a graphite-monochromatized Mo-K α radiation ($\lambda = 0.71073 \text{ \AA}$). The crystals were positioned at 40 mm from the CCD, and the diffraction spots were measured using a counting time of 15 s. Data reduction and multi-scan absorption were carried out using the APEX II program suite (Bruker, 2007). The crystal structures were solved by direct methods with the SIR97 program¹ and refined using full-matrix least squares with SHELXL-97.² Anisotropic thermal parameters were used for all non-H atoms. All other calculations were performed using the programs WinGX3³ and PARST.⁴ Final R-values, together with selected refinement details, are given in Table S1.†

References

- 1 A. Altomare, M. C. Burla, M. Camalli, G. L. Cascarano, C. Giacovazzo, A. Guagliardi, A. G. G. Moliterni, G. Polidori, R. Spagna, *J. Appl. Crystallogr.* 1999, **32**, 115-119.
- 2 G. M. Sheldrick, *Acta Crystallogr. A.* 2008, **64**, 112–122.
- 3 L.J. Farrugia, *J. Appl. Crystallogr.* 1999, **32**, 837.
- 4 M. Nardelli, *J. Appl. Crystallogr.* 1995, **28**, 659.

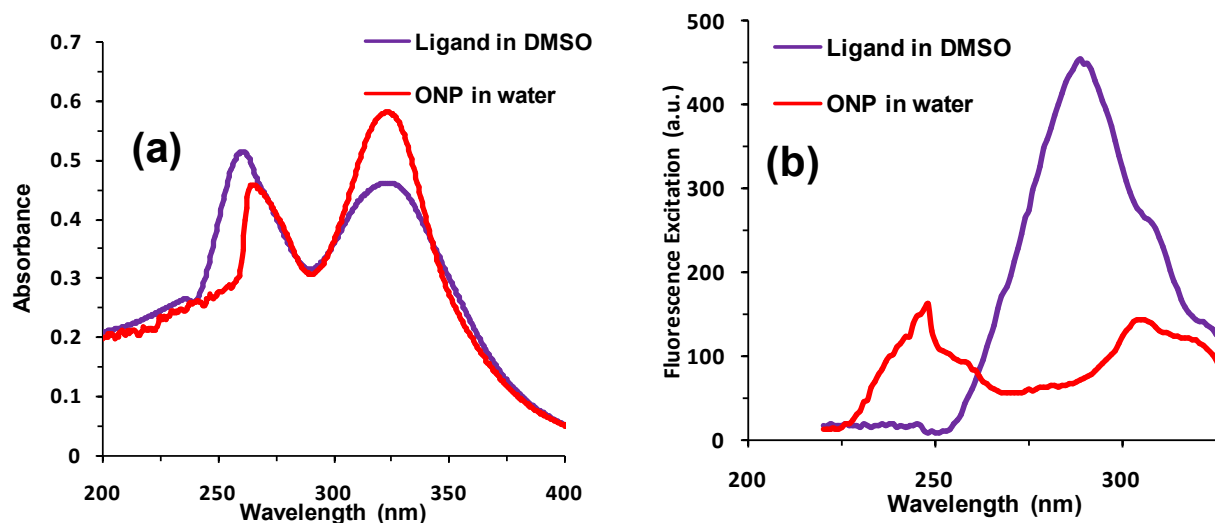


Figure S1. (a) The absorbance and (b) the excitation spectra of compound 1 (5 μM) in DMSO and its nanoparticles, ONP (5 μM) in water.

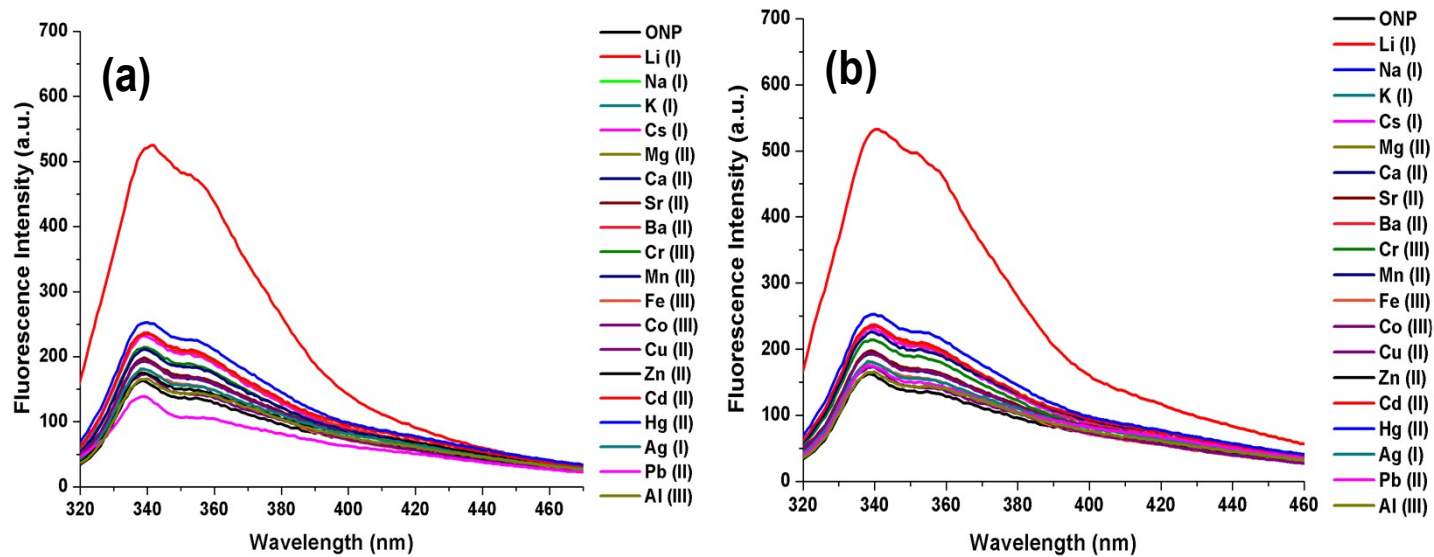


Figure S2. Changes in emission profile of ONP (5 μM) in water upon addition of 50 μM of particular metal nitrate salts (a) in absence of buffer (b) in presence of HEPES buffer, pH 7.4.

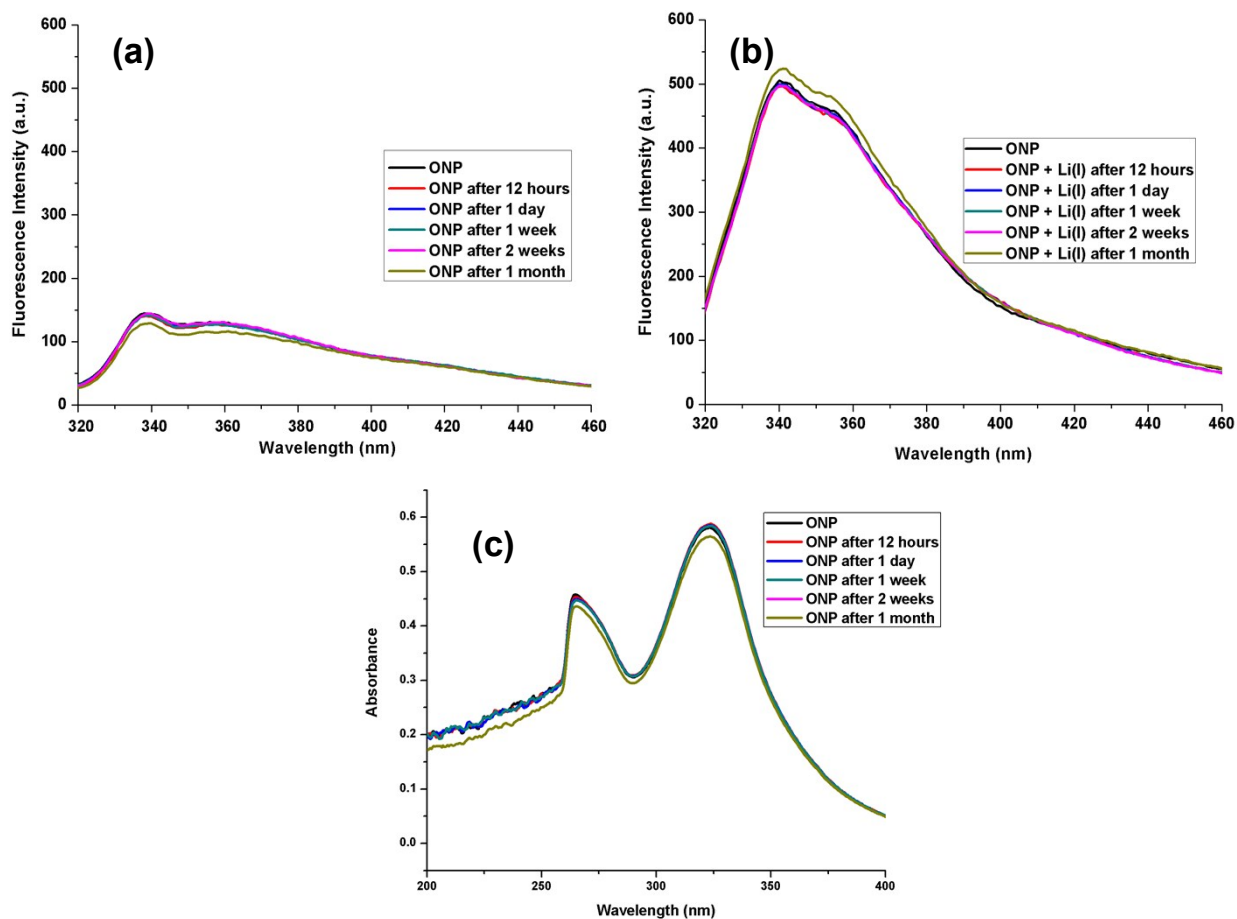


Figure S3. Fluorescence spectra of ONP (a) before Li (I) binding (b) after Li (I) binding at different time intervals. (c) Absorbance spectra of ONP at different time intervals.

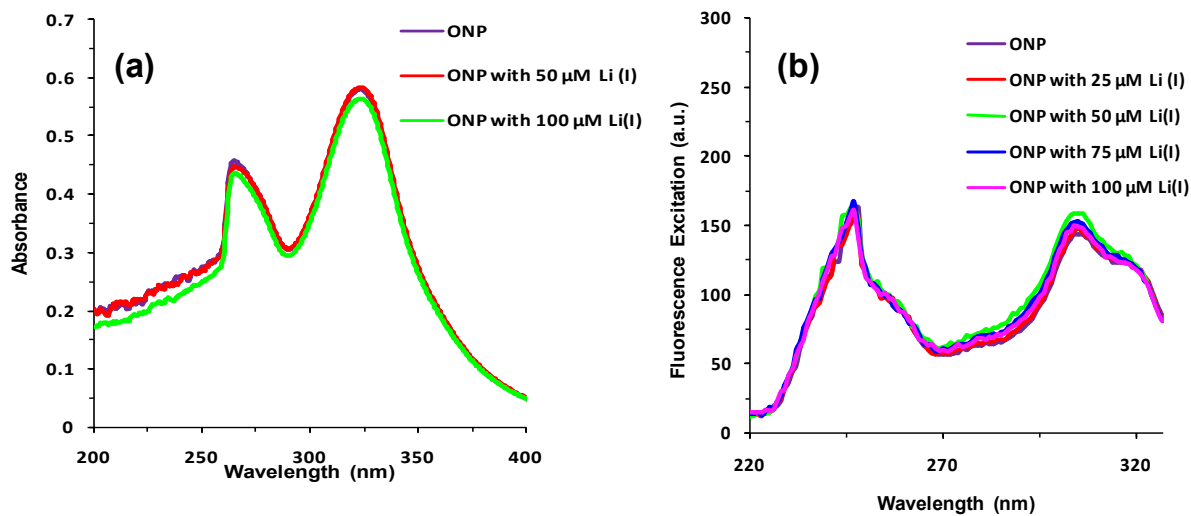


Figure S4. (a) Absorbance spectra of ONP upon titration with Li (I); (b) Excitation spectra of ONP upon titration with Li (I)

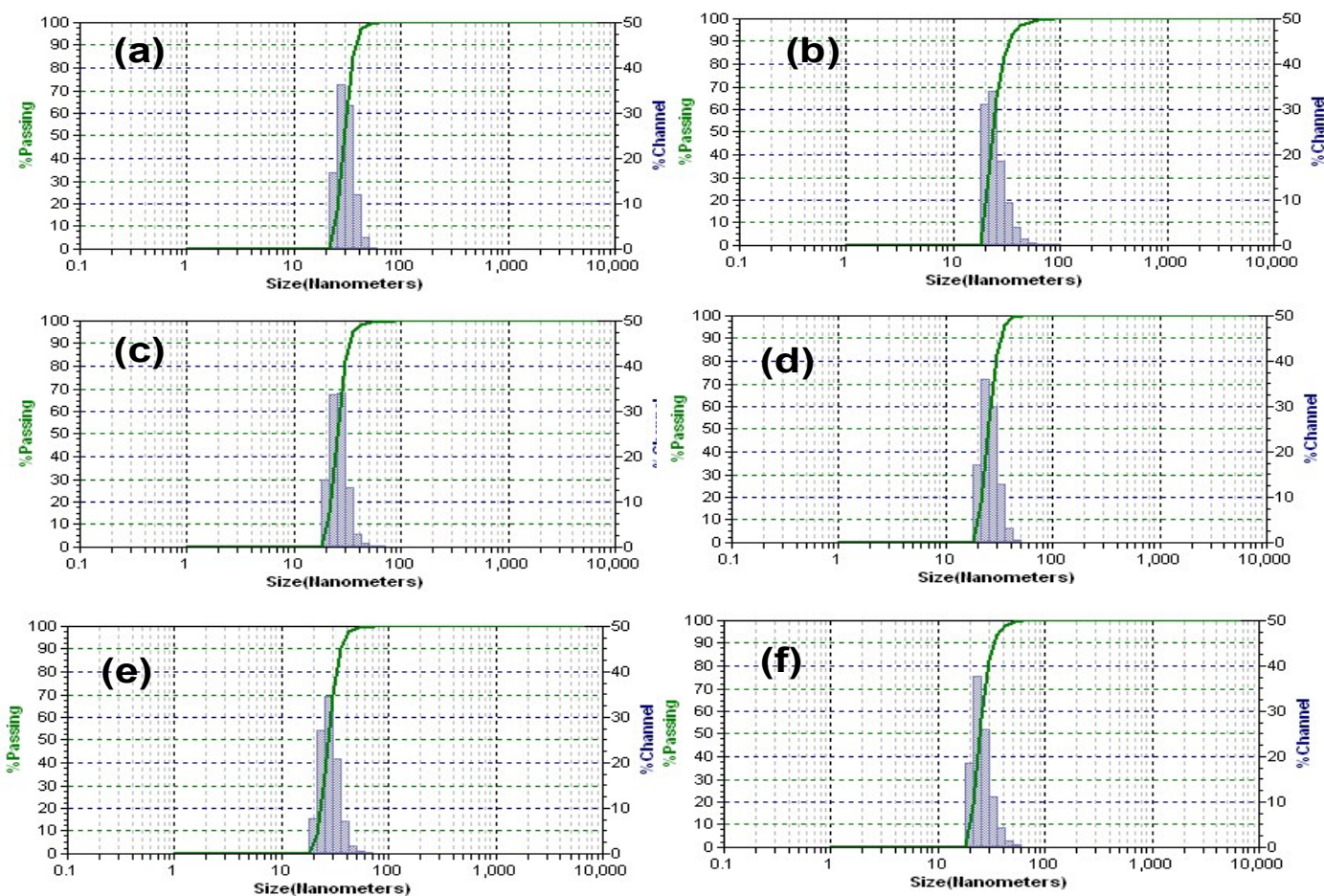


Figure S5. DLS histogram of ONP on interaction with (a) Li (I), 30 nm (b) Cs (I), 25 nm (c)Cr (III), 26nm (d) Al (III), 25 nm (e) Zn (II), 26 nm.

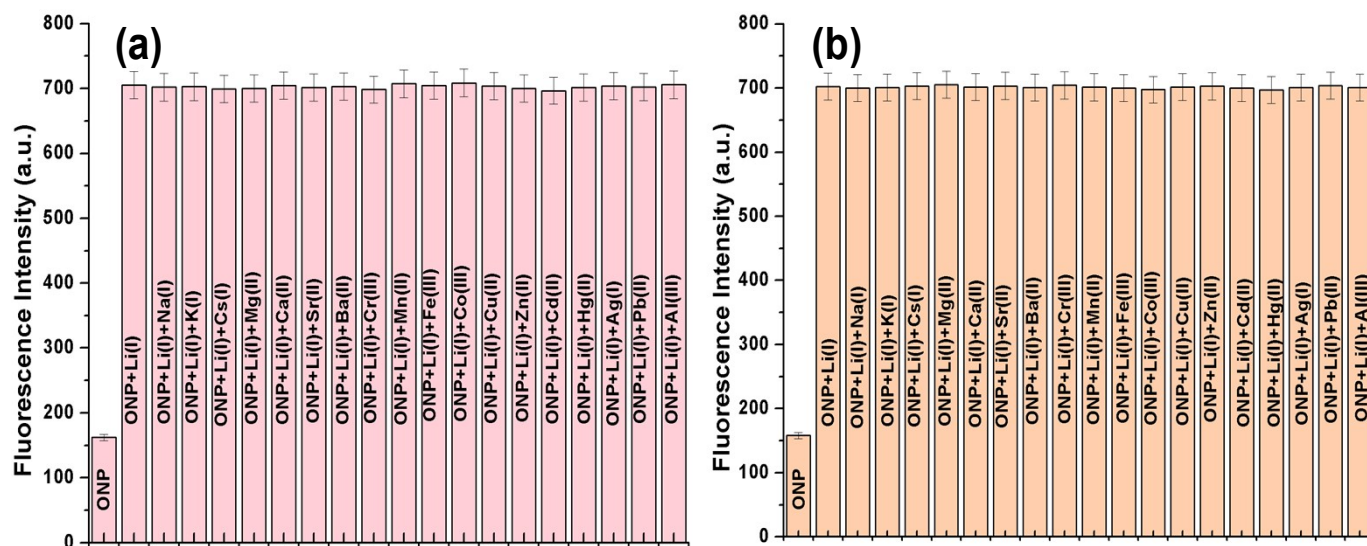


Figure S6. Competitive experiment (a) in absence of buffer (b) in presence of HEPES buffer, pH 7.4.

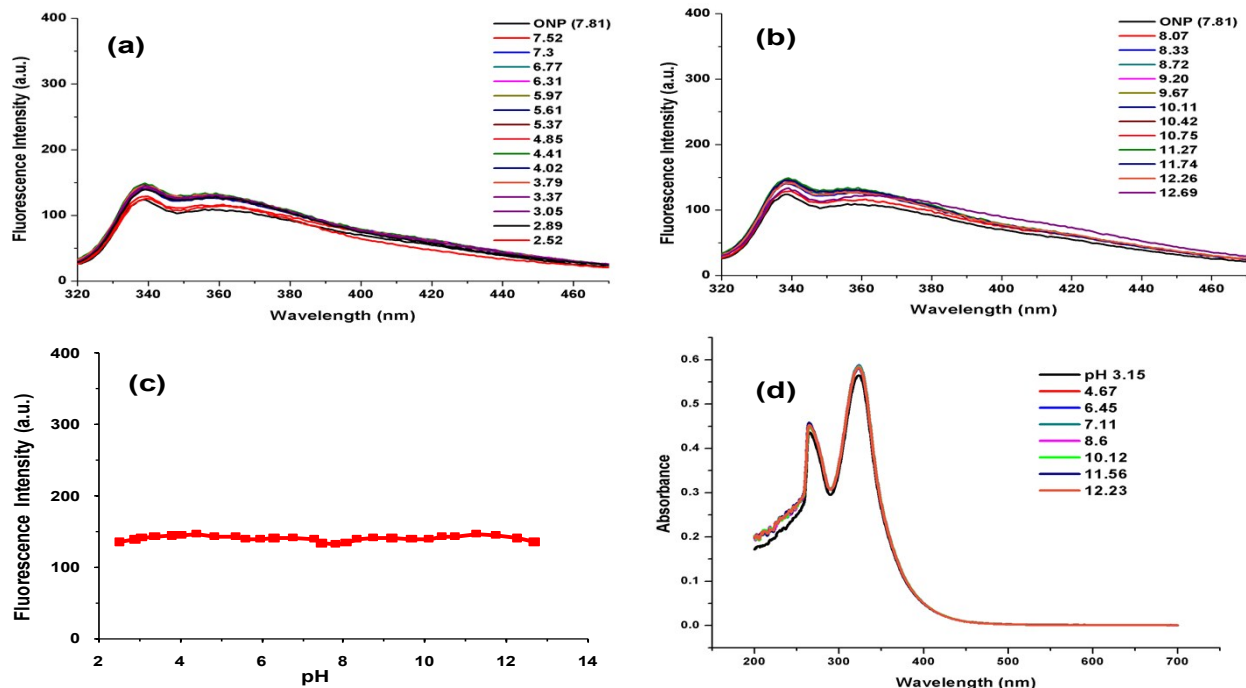


Figure S7. Fluorescence spectra of ONP at different pH values (a) acidic medium (b) basic medium (c) Fluorescence intensity vs pH profile (d) Absorbance spectra of ONP at different pH values.

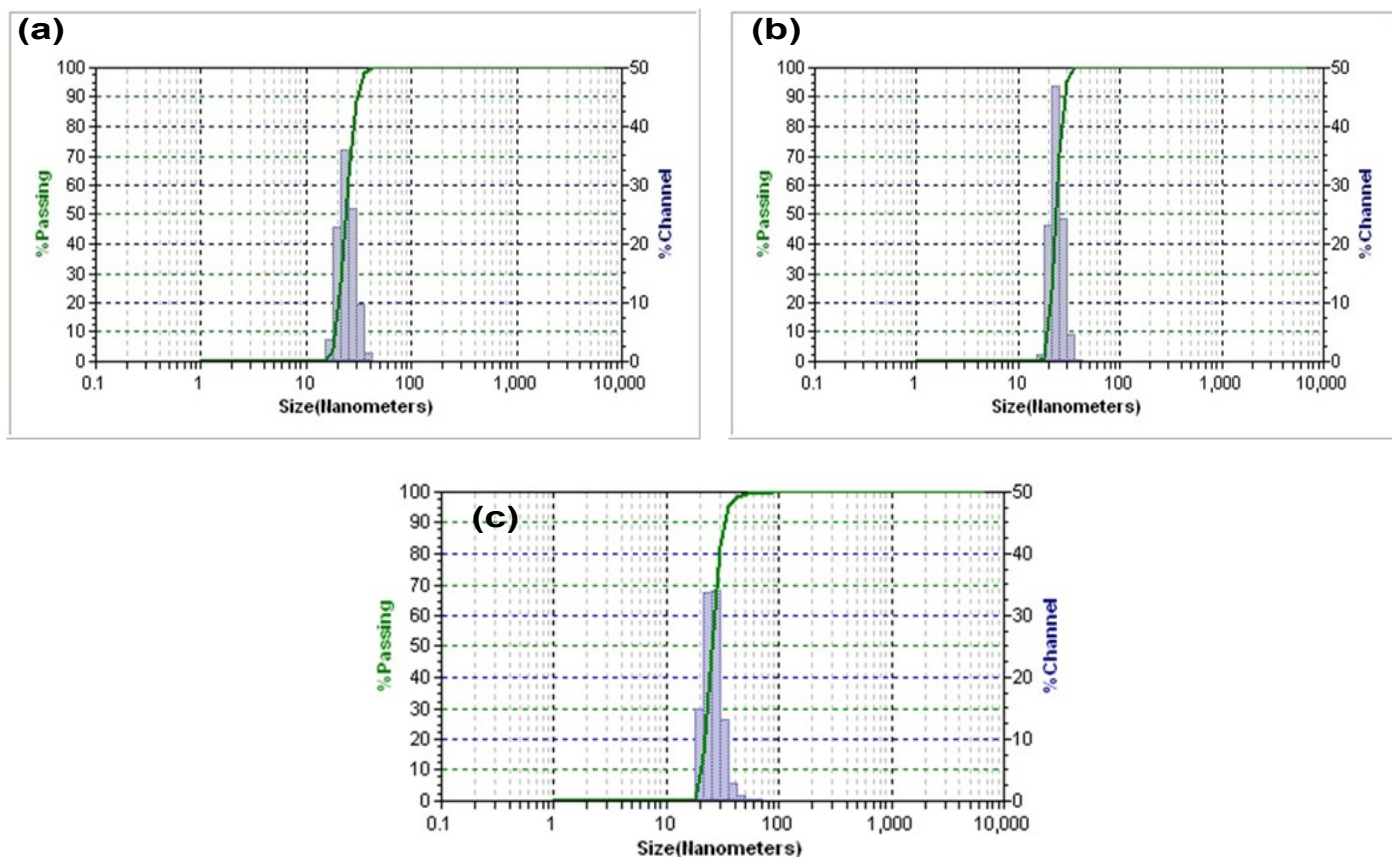


Figure S8. (a) DLS at pH=4.1, 25nm (b) DLS at pH= 8, 23nm (c) DLS at pH= 11, 25nm

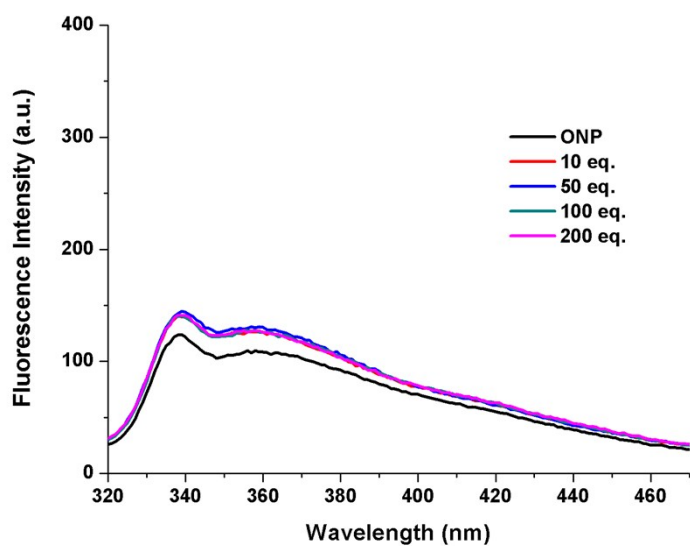


Figure S9. Fluorescence spectra of **ONP** on addition of different concentrations of tetrabutylammonium perchlorate to evaluate the salt effect.

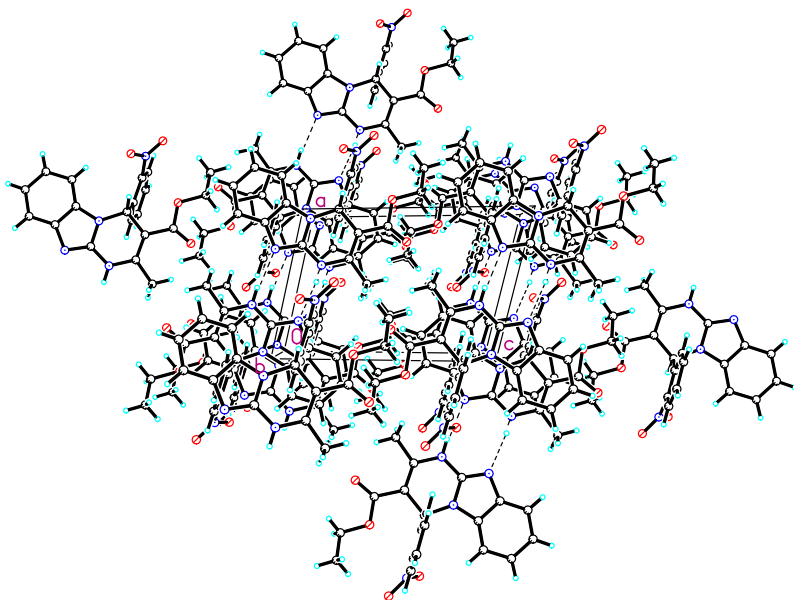


Figure S10. Packing diagram of 1.

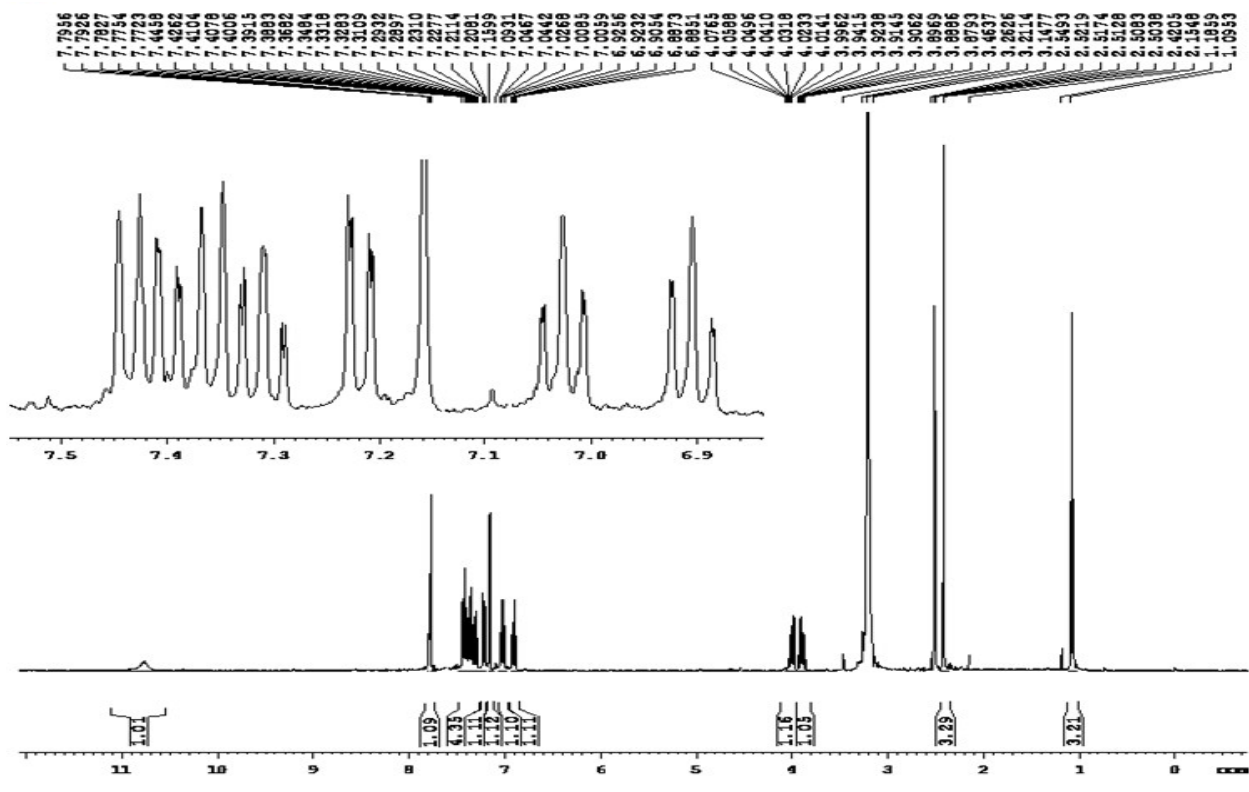


Figure S11. (a) ¹H-NMR of compound 1.

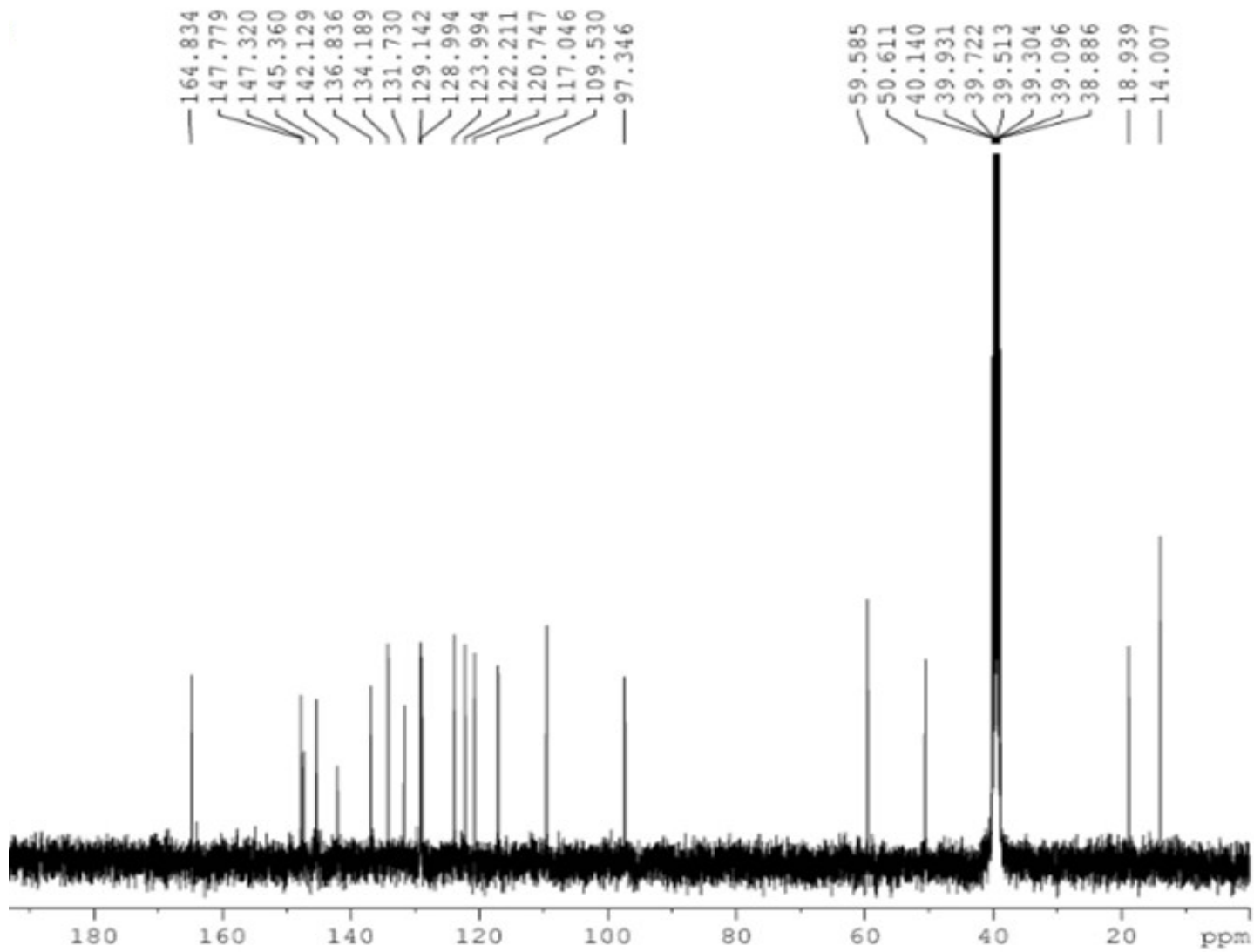


Figure S11. (b) ^{13}C -NMR of compound 1.

Table 1. Crystal data and structure refinement for 1.

Identification code	1
Empirical formula	C ₂₀ H ₁₈ N ₄ O ₄
Formula weight	378.38
Temperature	293(2) K
Diffractometer used	Bruker
Radiation used, Wavelength	MoK α , 0.71073 Å
Crystal system, Space group	Triclinic, P $\bar{1}$
Unit cell dimensions	a = 7.8274(3) Å
	b = 11.2215(5) Å
	c = 11.4253(5) Å
Volume	878.51(6) Å ³
Z, Calculated Density	2, 1.430 Mg/m ³
Absorption coefficient	0.102 mm ⁻¹
F(000)	396
Theta range for data collection	2.39 to 24.99°.
Index ranges	-9≤h≤9, -13≤k≤13, -13≤l≤13
Reflections collected	18207
Independent reflections	3097 [R(int) = 0.0312]
Refinement method	Full-matrix least-squares on F ²
Data / restraints / parameters	3097 / 1 / 254
Goodness-of-fit on F ²	1.036
Weighting scheme	1/[σ^2 (Fo ²)+(0.0965P) ² +0.37P], P=(max(F _o ² ,0)+2*F _c ²)/3
Data to parameter ratio	12.19:1
Final R indices, 2422 reflections [I>2 σ (I)]	R1 = 0.0578, wR2 = 0.1590
R indices (all data)	R1 = 0.0734, wR2 = 0.1691
Largest diff. peak and hole	0.258 and -0.509 e.Å ⁻³

Table 2. Bond lengths [Å] for 1.

O(1)-C(18)	1.203(3)
O(2)-C(18)	1.343(3)
O(2)-C(19)	1.447(4)
O(3)-N(4)	1.200(3)
O(4)-N(4)	1.197(3)
N(1)-C(7)	1.313(3)
N(1)-C(1)	1.399(3)
N(2)-C(7)	1.358(3)

N(2)-C(6)	1.397(3)
N(2)-C(8)	1.468(3)
N(3)-C(7)	1.360(3)
N(3)-C(10)	1.373(3)
N(3)-H(3A)	0.8600
N(4)-C(13)	1.471(4)
C(1)-C(2)	1.387(3)
C(1)-C(6)	1.395(3)
C(2)-C(3)	1.386(4)
C(3)-C(4)	1.381(4)
C(4)-C(5)	1.386(4)
C(5)-C(6)	1.385(3)
C(8)-C(9)	1.523(3)
C(8)-C(12)	1.538(3)
C(9)-C(10)	1.352(3)
C(9)-C(18)	1.470(3)
C(10)-C(11)	1.499(3)
C(12)-C(17)	1.385(3)
C(12)-C(13)	1.392(3)
C(13)-C(14)	1.381(4)
C(14)-C(15)	1.353(5)
C(15)-C(16)	1.377(5)
C(16)-C(17)	1.372(4)
C(19)-C(20)	1.436(6)

C(18)-O(2)-C(19)	114.6(3)
C(7)-N(1)-C(1)	103.35(17)
C(7)-N(2)-C(6)	105.43(17)
C(7)-N(2)-C(8)	126.03(17)
C(6)-N(2)-C(8)	127.93(17)
C(7)-N(3)-C(10)	121.15(18)
O(4)-N(4)-O(3)	121.0(3)
O(4)-N(4)-C(13)	120.6(2)
O(3)-N(4)-C(13)	118.4(3)
C(2)-C(1)-C(6)	119.7(2)
C(2)-C(1)-N(1)	129.8(2)
C(6)-C(1)-N(1)	110.52(18)
C(3)-C(2)-C(1)	117.9(2)
C(4)-C(3)-C(2)	121.9(2)
C(3)-C(4)-C(5)	121.1(2)
C(6)-C(5)-C(4)	116.9(2)

C(5)-C(6)-C(1)	122.6(2)
C(5)-C(6)-N(2)	132.0(2)
C(1)-C(6)-N(2)	105.38(17)
N(1)-C(7)-N(2)	115.30(18)
N(1)-C(7)-N(3)	125.45(19)
N(2)-C(7)-N(3)	119.24(19)
N(2)-C(8)-C(9)	108.53(17)
N(2)-C(8)-C(12)	108.84(16)
C(9)-C(8)-C(12)	111.47(18)
C(10)-C(9)-C(18)	121.0(2)
C(10)-C(9)-C(8)	122.4(2)
C(18)-C(9)-C(8)	116.6(2)
C(9)-C(10)-N(3)	121.6(2)
C(9)-C(10)-C(11)	126.1(2)
N(3)-C(10)-C(11)	112.3(2)
C(17)-C(12)-C(13)	115.8(2)
C(17)-C(12)-C(8)	117.90(19)
C(13)-C(12)-C(8)	126.3(2)
C(14)-C(13)-C(12)	122.1(2)
C(14)-C(13)-N(4)	115.3(2)
C(12)-C(13)-N(4)	122.6(2)
C(15)-C(14)-C(13)	120.3(3)
C(14)-C(15)-C(16)	119.2(3)
C(17)-C(16)-C(15)	120.3(3)
C(16)-C(17)-C(12)	122.3(2)
O(1)-C(18)-O(2)	121.5(3)
O(1)-C(18)-C(9)	127.2(3)
O(2)-C(18)-C(9)	111.2(2)
C(20)-C(19)-O(2)	109.6(4)